2016

Knee Internal Forces in Moderate Squat Exercise

Dumitru I. Caruntu
The University of Texas Rio Grande Valley, dumitru.caruntu@utrgv.edu

Jose Mario Salinas
The University of Texas Rio Grande Valley

Recommended Citation

Caruntu, DI, & Salinas, JM. "Knee Internal Forces in Moderate Squat Exercise." Proceedings of the ASME 2016 International Mechanical Engineering Congress and Exposition. Volume 3: Biomedical and Biotechnology Engineering. Phoenix, Arizona, USA. November 11–17, 2016. V003T04A054. ASME. https://doi.org/10.1115/IMECE2016-66626

AKNOWLEDGEMENTS

This work has been sponsored partially by the San Luis Potosí Autonomous University (UASLP) through the academic staff funds *UASLP-CA-78 and the Cooney-Jackman Endowment at Gannon University.

REFERENCES

[1] Evandro M. Ficanha, Guilherme Ribeiro and Mohammad Rastgaar Aagaah, "Instrumented Walkway for Estimation of the Ankle Impedance in Dorsiflexion-Plantarflexion and Inversion-Eversion During Standing and Walking," Proceedings of the ASME 2015 Dynamic Systems and Control Conference DSCC 2015 October 28-30, 2015, Columbus, Ohio, USA.

[2] Chavez-Romero Raul, Cardenas Antonio, Rendon-Mancha Juan Manuel, Vernaza Karinna M. and Piovesan Davide, "Inexpensive Vision-Based System for the Direct Measurement of Ankle Stiffness during Quiet Standing," ASME. J. Med. Devices. 2015; Vol 9

[3] Coronado Enrique, Chavez-Romero Raul, Cardenas Antonio, Piovesan Davide "Combining Genetic Algorithms and Extended Kalman Filter to Estimate Ankle's Muscle-Tendon Parameters", Proceedings of the ASME 2015 Dynamic Systems and Control Conference DSCC 2015 October 28-30, 2015, Columbus, Ohio, USA.

[4] Segura-Alvarado Mauricio E, Coronado Enrique, Maya Mauro, Cardenas Antonio and Piovesan Davide, "Analysis of recoverable falls via Microsoft Kinect: Identification of third-order ankle dynamics," J. Dyn. Sys., Meas., Control. 2016.

[5] Rendon-Mancha J.M., García Romero M. A., Cárdenas Antonio, Lara Bruno, Gonzalez-Galván Emilio, "Robot Positioning using Camera-Space Manipulation with a Linear Camera Model," IEEE Transactions on Robotics,Vol 26(4), pp. 726-733 Aug. 2010.

[6] Z. Zhengyou, "A flexible new technique for camera calibration," Pattern Analysis and Machine Intelligence, IEEE Transactions on, vol. 22, pp. 1330-1334, 2000.

[7] R. Hartley and A. Zisserman, Multiple View Geometry in Computer Vision: Cambridge University Press, 2003.

[8]. Piovesan, D., Pierobon, A., DiZio, P., Lackner, J.R. 2012. Measuring Multi-Joint Stiffness during Single Movements: Numerical Validation of a Novel Time-Frequency Approach. PloS one, Vol. 7, p. e 33086.

[9]. Chavez-Romero, C.R., Cardenas A., R. Piovesan, D. 2014. Viscoelastic properties of the ankle during quiet standing via raster images and EKF. Signal Processing in Medicine and Biology Symposium, 2014 IEEE, pp. 1-5.

[10] Simon, D. 2006. Optimal State Estimation, Kalman, H1, and Nonlinear Approaches. New Jersey: John Wiley & Sons, Inc. 2006.

Proceedings of the ASME 2016 International Mechanical Engineering Congress and Exposition
IMECE2016
November 11-17, 2016, Phoenix, Arizona, USA

IMECE2016-66626

KNEE INTERNAL FORCES IN MODERATE SQUAT EXERCISE

Dumitru I. Caruntu
Mechanical Engineering Department
The University of Texas Rio Grande Valley
Edinburg, Texas 78539

Jose Mario Salinas
Mechanical Engineering Department
The University of Texas Rio Grande Valley
Edinburg, Texas 78539

ABSTRACT

This paper deals with internal forces of human knee during moderate squat exercise. The moderate squat exercise consists of a descending phase from standing to the lowest position (largest flexion angle) in which no significant contact between thigh and calf occurs, and an ascending phase back to standing position. This research predicts the internal forces such as muscle forces, contact forces, and ligamentous forces. The ligamentous structures in this research consist of Anterior Cruciate Ligament (ACL), Posterior Cruciate Ligament (PCL), Lateral Collateral Ligament (LCL), and Medial Collateral Ligament (MCL). The ligaments are modeled as nonlinear elastic strips (they do not carry compression forces). An optimization technique was used to determine the muscle and contact forces present in the knee during the squat exercise.

INTRODUCTION

The knee joint is the largest joint of the body. Unlike other joints that are formed by two bones, the knee is made up of three bones: the femur, patella, and tibia [1]. Although the knee is usually thought of as being a single joint, it actually consists of two joints working in concert to allow movement and provide mechanical support. The two joints that make up the knee are the patello-femoral joint, and tibio-femoral joints [1].

Joint stability in the knee is achieved through the collaboration of two sets of ligaments, the collateral ligaments and the cruciate ligaments. The collateral ligaments are found outside the articular capsule and consist of the medial and lateral collateral ligaments; these extra-capsular ligaments help prevent lateral and medial displacement of the tibia when the knee is extended [1]. Moreover, the lateral collateral ligament (LCL) runs from the lateral epicondyle of the femur to the head of the fibula. The medial collateral ligament (MCL) runs from the medial epicondyle of the femur to the medial condyle of tibia [1].

The cruciate ligaments are found inside the articular capsule and, as the name suggests, form a cross in the notch between the femoral condyles. The two cruciate ligaments are the anterior cruciate ligament (ACL) and the posterior cruciate ligament (PCL). The primary function of the ACL is to prevent knee hyperextension as well as forward sliding of the tibia with respect to the femur. The PCL's primary function is to prevent the backward displacement of the tibia in relation to the femur [1].

Cruciate and collateral ligaments are known to exhibit nonlinear viscoelastic properties. A nonlinear property of ligaments that is of particular interest in this paper is their nonlinear stress-strain curve. The nonlinear nature of the stress-strain curve of ligaments is due to the ligament's composition. Ligaments are made up of connective tissue, which in turn is made up of bundles of elastic and collagenous fibers. According to Butler et al. [2], the stress-strain curve for a typical ligament can be divided into three zones. Zone 1 is characterized by the uncoiling of collagenous fibers. Initially, the stiffness of the ligaments is attributed to the elastic fibers; however, as the ligament elongates and more collagen is uncoiled the stiffness of the ligament becomes more and more dependent on the collagenous fibers [2]. Moreover, the stiffness increases as the collagens uncoil and get aligned. This stress-strain relationship can be represented as a quadratic equation [2]. In zone 2, all of the collagen has been uncoiled, and the stiffness in the ligament is solely dependent on the collagen fibers. At this point, the stress-strain behavior is usually treated as a linear equation. Lastly, the collagen fibers begin to rupture in zone 3 and continue to rupture throughout the zone until the ligament fails completely [2].

Knee flexion and extension is achieved primarily by the antagonistic relationship of two groups of muscles. These two groups of muscle are commonly known as the quadriceps and the hamstrings. The quadriceps is subdivided into four muscles: rectus femoris, vastus lateralis, vastus medialis, and vastus intermedius. The primary function of the quadriceps is to extend the knee [3]. Furthermore, the hamstrings are located along the posterior side of the thigh, and consist of three muscles: biceps femoris, semitendinosus, and semimembranosus. The primary function of the hamstrings is to flex the knee [3]. Body movements and balance are achieved through the collaborate effort of muscles and ligaments.

Muscles and ligaments exert precise tension forces onto bones to produce smooth movements and maintain a stable posture.

The purpose of the investigation presented in this paper, was to determine the internal forces of the knee that develop during a moderate squat. The overall approach was to collect the kinematic and kinetic measurements experimentally using motion capture cameras and force plates, then apply the collected experimental data to a knee joint model to calculate the resulting internal forces. The mathematical model for the knee joint consisted of a 2-dimentional dynamic model that uses an optimization technique to determine the internal loads found in the knee. The internal loads determined by the 2-dimentional model consist of forces generated by muscles and contact points. Ligament forces are assumed to behave like rubber strings and are determined geometrically. Furthermore, the tibiofemoral contact is assumed to occur at a point that translates along the tibial plateau during the squat exercise and is identified geometrically using the experimentally measured kinematic data.

2-D DYNAMIC MODEL OF KNEE JOINT

A two-dimensional model was developed to calculate the ligament, muscle, and contact forces. Three bony structures are accounted for in this model, femur, tibia and patella. The bony structures are assumed to be rigid bodies. The tibiofemoral contact is assumed to occur at a point along the tibial plateau. The location of the contact point is calculated geometrically using the measured kinematic data. Both the cruciate (ACL and PCL) and the collateral ligaments (MCL and LCL) are included in this model.

The internal forces of the human knee consist of articular contact forces, i.e. tibio-femoral and patello-femoral contact forces, muscle forces in muscles such as the quadriceps muscle including rectus femoris and vasti muscles, the hamstrings muscle, and the gastrocnemius muscle. An inverse dynamic model is used to investigate the squat exercise. In inverse dynamics, the accelerations are experimentally determined, and then the internal forces are predicted through numerical simulations. The inverse dynamic model, which is an optimization procedure, consists of an objective function in which the sum of squares of internal forces is minimized, and both equality and inequality constraints. The equality constraints consist of equations of motion of the bony structures in the model. The inequality constraints consist of forces being greater than zero for tension forces in the muscles and articular contact forces. The experiments were conducted in the Biomechanics Laboratory (Director Dr. Dumitru Caruntu) at the University of Texas Rio Grande Valley. The human subject was a healthy male twenty three years old, 80 kg and 1.80 m. He went from standing position (zero flexion angle) to moderate squatting (about 120 degrees flexion angle), and back to the standing position. Markers on the human subject were located on bony landmarks such as ankle, tibial tuberosity, lateral knee condyle, and greater trochanter. The instrumentation recorded the motion of these markers during the exercise. With this data, the motion of the centers of mass of tibia and femur were determined, and then their accelerations calculated through numerical differentiation. At the same time the ground reaction forces were recorded. Both the kinematics and the ground reaction forces were recorded by a motion analysis system and two force plates, respectively. The accelerations of the centers of mass of femur and tibia, and the ground reaction forces were input data for the inverse dynamics model.

The cruciate and collateral ligaments are assumed to behave like elastic strings characterized by a quadratic force-elongation curve, for low elongations, and after reaching a particular threshold, characterized by a linear force-elongation curve [2]. Therefore, ligament forces can fall under one of three cases depending on the amount of strain the ligament has undergone [4]. The three cases and there corresponding equations are described below

CASE 1: If ligaments do not experience any strain ($\varepsilon_n \leq 0$), then the ligament force will be equal to zero.

$$F_{lig} = 0 \tag{1}$$

CASE 2: If the ligament strain falls between 0 and the linear threshold ($0 < \varepsilon_n < 2\varepsilon_o$), then the ligament force can be expressed by the following equation.

$$F_{lig} = K_{lig}\left(L_{lig} - SL_{lig}\right)^2 \tag{2}$$

CASE 3: If the ligament strain is greater than the linear threshold ($\varepsilon_n \geq 2\varepsilon_o$), then the ligament force can be expressed by the following equation.

$$F_{lig} = k_{lig}\left(L_{lig} - SL_{lig}\right) \tag{3}$$

where ε_n is the strain coefficient, $2\varepsilon_o$ is the strain threshold for the linear region, F_{lig} is the ligament force, k_{lig} is the elastic constant for the linear region, K_{lig} is the elastic constant for the quadratic region, and SL_{lig} is the ligament slack length. Figure 1 shows the free body diagram for ligament forces on femur and tibia.

Furthermore, the muscles that are included in the dynamic model are the following: quadriceps (*Fq*), hamstring (*Fh*), iliacus (*Fi*), rectus femoris (*Frf*), biceps femoris (*Fbfs* and *Fbfl*), gluteus (*Fg*), vastus (*Fv*), and gastrocnemius (*Fgas*). The contact forces that are included in the model consist of the x and y components for the contact point at the hip joint (*Fhx* and *Fhy*) and the x and y components for the tibiofemoral contact (*Fcx* and *Fcy*). These forces are illustrated on the free body diagrams shown in Figs. 2 and 3.

Anthropometric data was used to estimate the measurements for the tibial plateau [5] and the femoral head radius [6]. Other anatomical features that were obtained using anthropometric data include the center of mass for femur and tibia, the mass of the thigh, and the mass of the lower leg [7]. Furthermore, the right lateral condyle was assumed to have a circular shape. The radius and center of the right lateral condyle were selected by applying three assumptions. First, the center of the right lateral condyle was assumed to fall along the line that passes through both the marker that was placed on the right later condyle and the marker that was placed on the right greater trochanter of the femur. Second, it was assumed that if a perpendicular line with respect to the tibial plateau were drawn through the center of the right lateral condyle the line would stay within the tibial plateau for all flexion angles. Lastly, it was assumed that the resulting translation of a perpendicular line with respect to the tibial plateau would travel within 14 to 28 mm during the descending phase. This range was selected based on the average anterior/posterior translation of the femur relative to the tibia determined by [8] and [9].

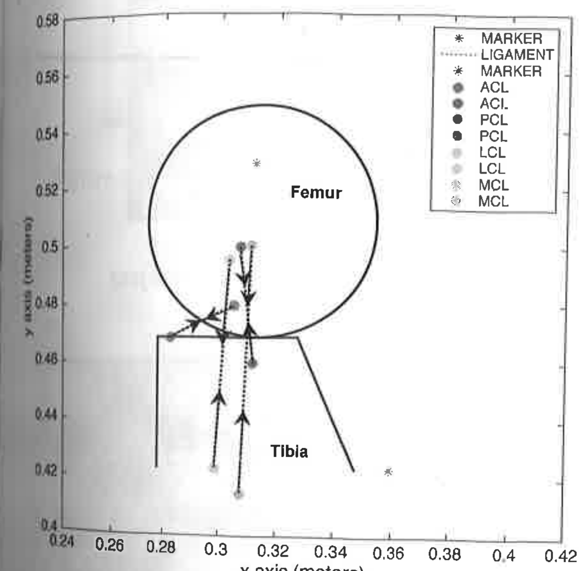

Figure 1: Free body diagram for ligament forces on femur and tibia.

Several assumptions were made when deriving the equations of motion. First, forces generated by the biceps femoris (*Fbfs* and *Fbfl*), and the *y* component of the contact point found at the hip are assumed to be parallel to the length of the femur. Second, forces produced by the quadriceps (*Fq*), gastrocnemius (*Fgas*), and the *y* component for the tibiofemoral contact point are assumed to be parallel to the length of the tibia. Third, forces generated by the gluteus (*Fg*) and iliacus (*Fi*) are assumed to always be pointing up along the global *y*-axis.

Lastly, the *x* component for the contact point at the hip is assumed to be perpendicular to the longitudinal axis of the femur. The equations of motion of femur and tibia used for the optimization process are the following

$$\sum F_{xf} = m_f \times a_{xCf}$$
$$\sum F_{yf} = m_f \times a_{yCf} \tag{4}$$

$$\sum M_{Cf} = I_f \times a_f$$

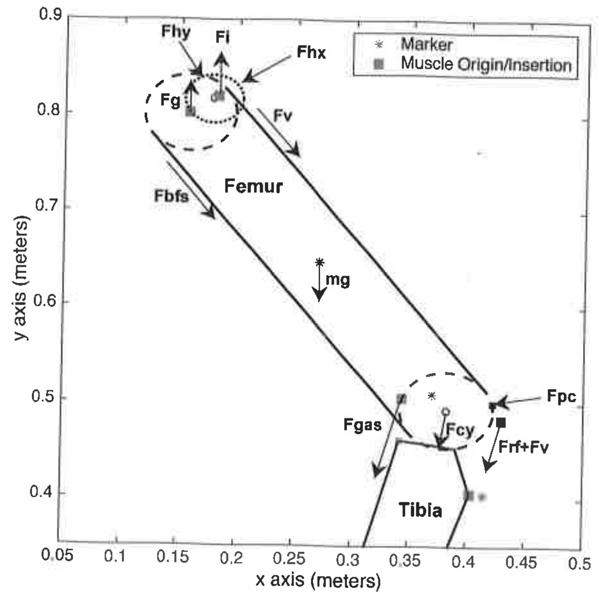

Figure 2: Free body diagram for muscle and contact forces of femur.

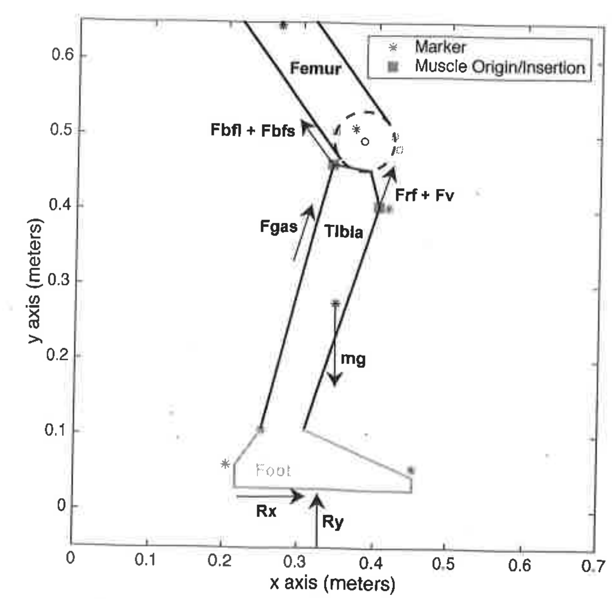

Figure 3: Free body diagram for muscle and ground reaction forces of tibia.

$$\sum F_{xt} = m_t \times a_{xCt}$$
$$\sum F_{yt} = t \times a_{yCt} \tag{5}$$

Copyright © 2016 by ASME

$$\sum M_{Ct} = I_t \times a_t$$

where F_{xf} and F_{yf} are the sum of the forces along the x and y axes, a_{xCf}, a_{yCf}, and a_f describe the acceleration of the femur, M_{Cf} is the sum of the moments about the center of mass of the femur, m_f is the mass of the femur, and I_f is the moment of inertia of the femur; and where F_{xt} and F_{yt} are the sum of the forces along the x and y axes, a_{xCt}, a_{yCt}, and a_t describe the acceleration of the tibia, M_{Ct} is the sum of the moments about the center of mass of the tibia, m_t is the mass of the tibia, and I_t is the moment of inertia of the tibia.

Unlike the ligament forces, muscle and contact forces are determined through an optimization process. Using an optimization technique is necessary because the number of muscle and contact forces that are being solved is higher than the number of equations derived from the dynamic system [7]. In addition to the equations of motion, the optimization method also requires a set of inequality constraints in order to come up with a solution. Two assumptions about muscle forces and contact forces are expressed by the inequality constraints. First, muscles are assumed to only exhibit tensile forces and thus the value for muscle forces must be positive; and second, the x component of the tibiofemoral contact point is assumed to be equal to zero.

EXPERIMENTAL PROTOCOL

An integrated system consisting of motion capture cameras and force plates were used to collect the experimental data. Unlike traditional cameras, motion capture systems, like the one used to collect the kinematic measurements in this paper, do not produce colored images; instead, the motion capture cameras generate a 3-dimensional spatial image in which the location of specific markers is tracked. Figure 4 shows the 3-dimensional image produced by the motion capture cameras. Moreover, the equipment setup consisted of ten Vicon MX T-Series cameras (motion capture system) surrounding two AMTI force plates. The ten Vicon MX T-Series cameras and the two AMTI force plates were used to collect kinematic and kinetic measurements, respectively. The equipment used during the experiments is shown in Fig. 5.

Vicon MX T-Series cameras gather the kinematic measurements by tracking reflective markers that are placed on the subject. Reflective markers were placed in specific landmarks on the hip, thigh, and lower leg as shown on Fig. 6. After markers were placed, the test subject was required to stretch out and perform 5 practice squats in order to loosen up the muscles and ensure that the placement of the markers does not interfere with the subject's ability to perform the exercise. The experiment required the subject to perform 5 sets each consisting of 10 moderate squats. Subjects were allowed to rest 3 minutes between sets. Squats were executed keeping the heels on the ground. Moreover, the subject was required to take between 2.5 and 3 seconds to perform the squat as well as to maintain the standing position for at least half a second.

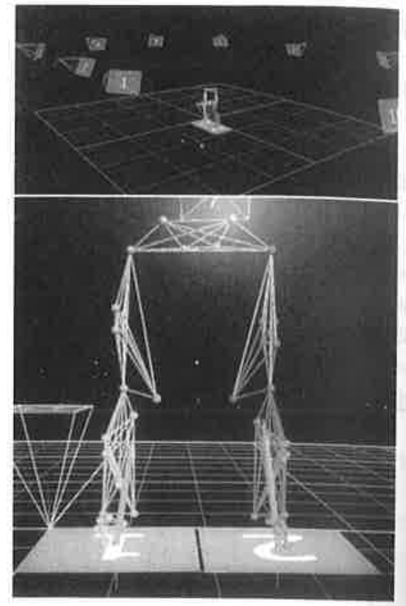

Figure 4: 3D image of test subject

Figure 5: Image of AMTI force plates (left) and Vicon MX T-Series cameras (middle and right)

RESULTS

Kinematic and kinetic measurements were collected and applied to the previously described 2D dynamic model in order to determine the internal forces of the knee. Results were plotted using MATLAB and are shown on figures 7-13.

The subject's flexion angle during the squatting exercise is shown In Fig. 7. During the experiment the minimum flexion angle was considered to be the standing position. Moreover, the value for the minimum flexion angle was approximately 5 degrees. Also, note that the value for the maximum flexion angle was approximately 112 degrees.

The distance between the tibiofemoral contact point and the posterior edge of the tibial plateau is shown in Fig. 8. Results for this distance were compared to data available in the literature [9]. Furthermore, data obtained from the literature was assumed to have the same initial distance as that determined experimentally. Note that the displacement for the tibiofemoral contact point from the standing position to the

maximum flexion is approximately the same for both sets of data.

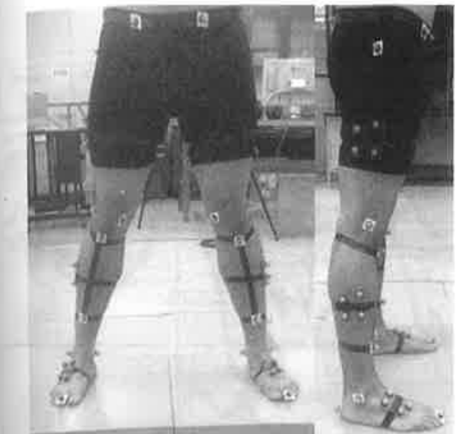

Figure 6: Image of test subject before performing the squat exercise.

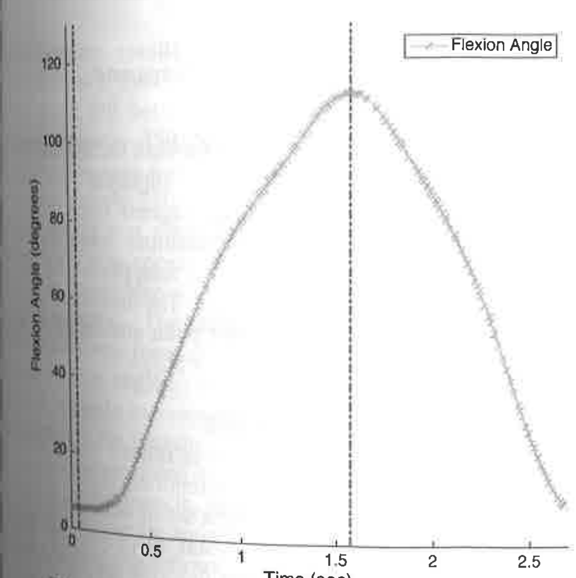

Figure 7: Flexion angle as a function of time.

Figure 9 show the ground reaction forces that were collected using the AMTI force plates.

Figures 10 and 11 compare the ligament forces experienced during the squatting exercise for the experiment presented on this paper to the ligament forces determined by [10] and [11]. The two main ligament forces observed were produced by the ACL and PCL. Out of the two forces the PCL displayed the higher force reaching a peak of 1740 N at a flexion angle of 109 degrees. The ACL produced a significantly smaller maximum force of approximately 640 N during the standing position. Although the magnitude of the ligament forces did not match, the overall trend is shared by [10].

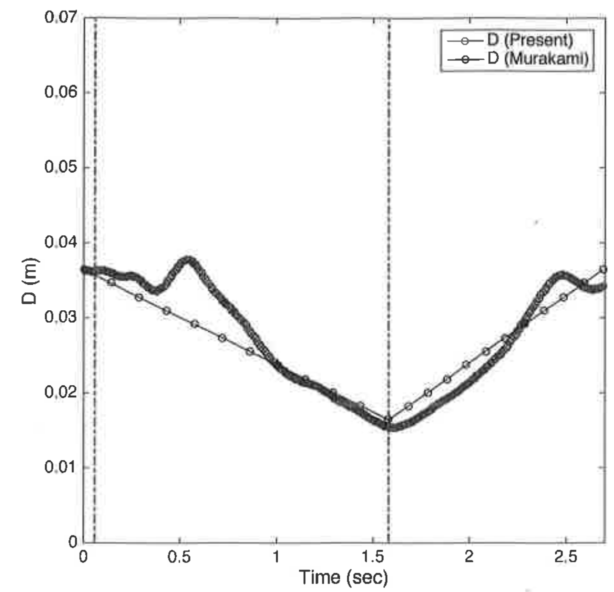

Figure 8: Distance between the tibiofemoral contact point and the posterior edge of the tibial plateau.

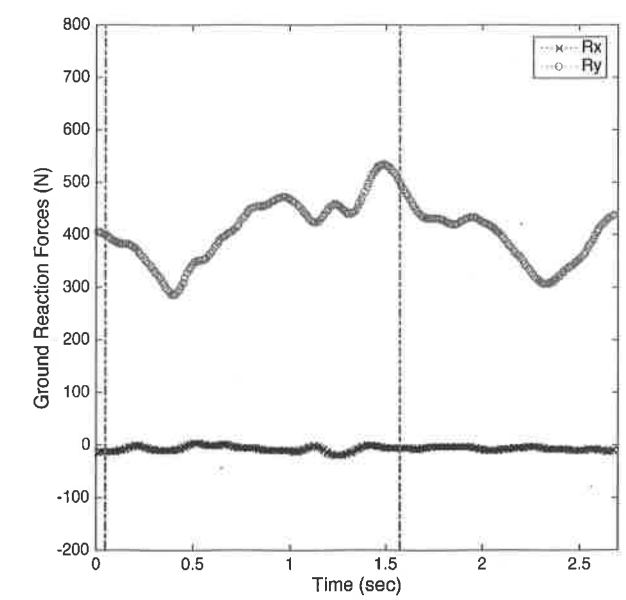

Figure 9: Ground reaction forces versus time for a moderate squat exercise.

The PCL force does however, fall between the values obtained by [10] and [11] suggesting that the determined value is within an acceptable range. Furthermore, no forces were observed for the MCL and a small force was observed for the LCL when the subject was in the standing position. Note that the data points for [10] and [11] are discontinuous because the flexion angles were lower than what is presented in this paper. Also, measurements for the descending phase are given in [10].

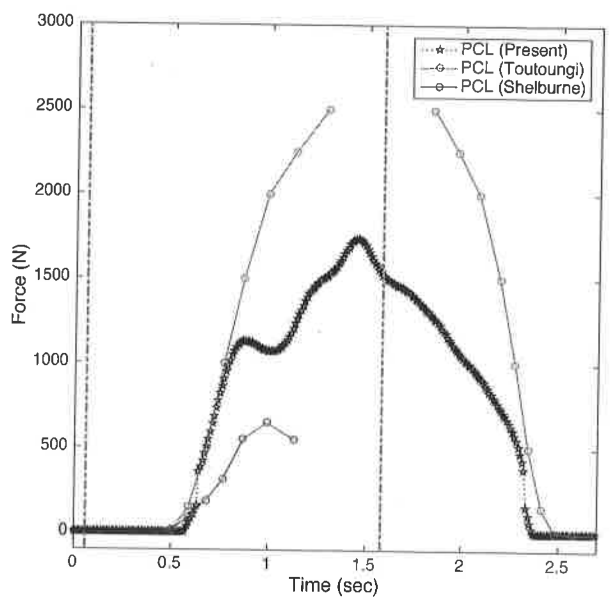

Figure 10: Comparison of PCL forces.

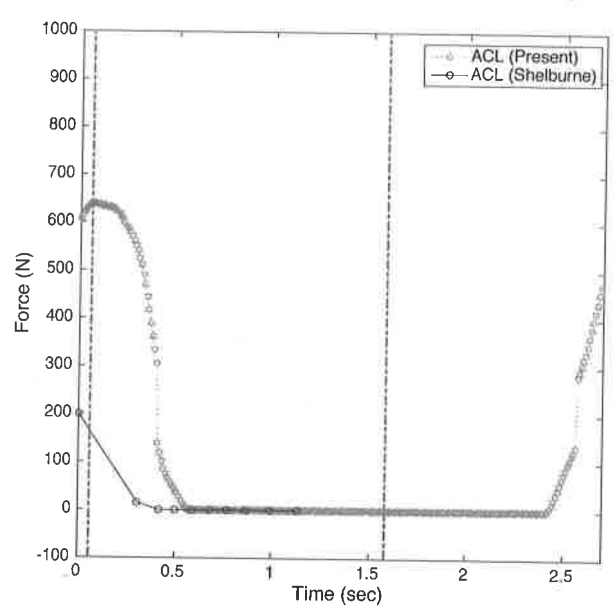

Figure 11: Comparison of ACL forces.

Tensile forces generated by the quadriceps, hamstring, and gastrocnemius are shown Fig. 12. Out of the three muscles, the quadriceps displayed the highest force, which was 1682 N and occurred when the subject was at 109 degrees. The hamstring reached a force of 1278 N at approximately 105 degrees; and lastly the gastrocnemius got a maximum force of 497 N in the standing position. Figure 12 also compares the quadriceps and hamstring forces that were determined experimentally to those obtained by [10]. The magnitudes of the forces do not seem to agree, however, the quadriceps do begin to increase at the same flexion angle. Moreover, the quadriceps force is greater than the hamstrings at high flexion angles for both sets of results.

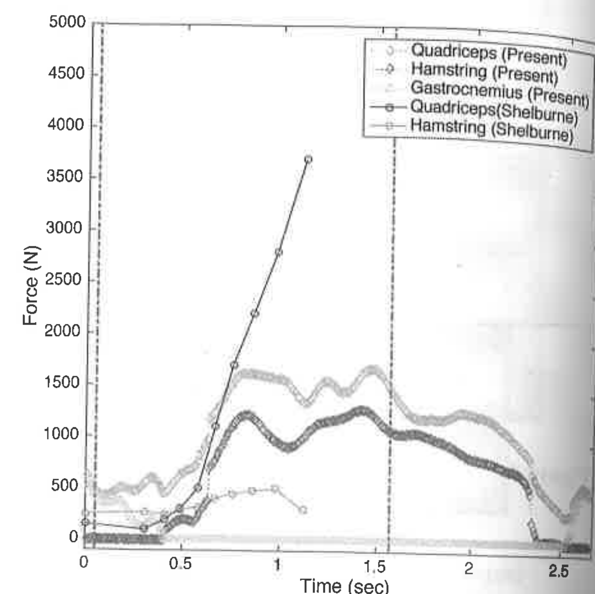

Figure 12: Comparison of quadriceps and hamstring forces.

Figure 13 shows the contact forces for both the hip and the tibiofemoral contact point. The y-component for the tibiofemoral contact point displayed the highest force overall during the squatting exercise. The maximum force for the tibiofemoral contact point was 2689 N and took place when the subject was at the maximum flexion angle. The maximum force for the x-component for the hip contact point also occurred at the maximum flexion angle and was 2139 N.

DISCUSSION AND CONCLUSIONS

Ligament, muscle, and contact forces related to the knee when performing a moderate squat are reported in this paper. Ligament forces were calculated using a set of conditions that are dependent on the amount of strain displayed by the ligament. Physically, these conditions describe the ligaments as behaving like elastic strings. Mathematical equations are used to account for this behavior. Muscle and contact forces were determined using an optimization technique. During the optimization process muscles were assumed to only exhibit tensile forces. Results for both ligament and muscle forces were compared to previous studies in order to validate the presented dynamic model.

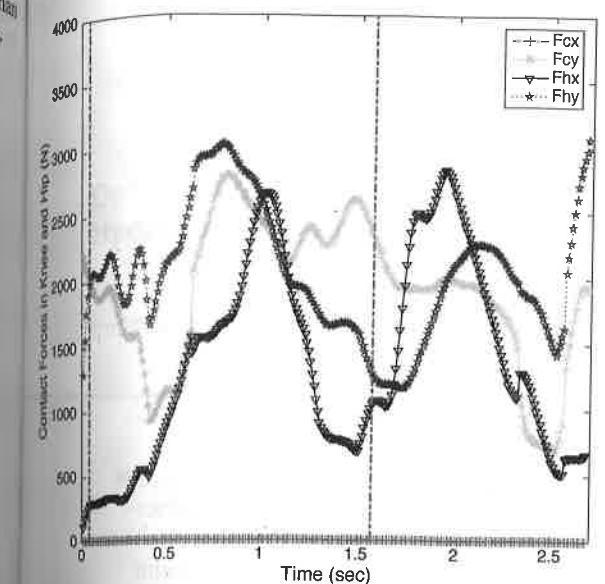

Figure 13: Contact forces for the hip and tibiofemoral contact point.

Furthermore, results were in agreement with data reported in the literature. The maximum PCL force (1740 N) calculated in this work fell between the PCL forces used for comparison (approximately 750 N and 2500 N). Only one source for comparison was found for the ACL and it was slightly lower (approximately 250 N) than what was obtained in this paper (640 N). It was also observed that the overall activity of the ligaments was consistent with data reported in the literature. Muscle forces also shared several features to those reported by other scientist. The most notable of these features being that the quadriceps force is greater than the hamstring force during high flexion angles. It was also observed that the quadriceps force began to increase around the same flexion angle as those reported in the literature.

A 2-dimensional dynamic model was developed in order to determine the muscle, ligament, and contact forces of the knee during a moderate squat. However, the proposed model does have several limitations, most of which are related to the way anatomical structures were modeled. In other words, aspects of the bone were assumed to be simple shapes. For example, the right lateral condyle was modeled as a circle and the tibial plateau was modeled as a flat surface. Another limitation is the way muscles were modeled. In some cases, the tensile force resulting from muscle contractions were assumed to point at a particular direction that is not entirely accurate; for example, the force produced by the iliacus and gluteus medius were assumed to always point up along the global y-axis.

ACKNOWLEDGEMENT

This work has been supported by the National Science Foundation CBET Division grant # 1126763.

REFERENCES

[1] Marieb, E. N., Hoehn, K., 2010, *Human Anatomy & Physiology (8th edition)*. Benjamin/Cummings. Redwood City. CA., Chap. 8

[2] Butler, D.L., Grood, E.S., Noyes, F.R., Zernicke, R.F., 1978. Biomechanics of ligaments and tendons. Exerc. Sports Sci. Rev. **6,** 125-181.

[3] Marieb, E. N., Hoehn, K., 2010, *Human Anatomy & Physiology (8th edition)*. Benjamin/Cummings. Redwood City. CA., Chap. 10

[4] Caruntu, D.I., Hefzy, M.S., 2004, 3-D Anatomically Based Dynamic Modeling of the Human Knee to Include Tibio-Femoral and Patello-Femoral Joints, ASME Journal of Biomechanical Engineering **126**(1), pp. 44-53.

[5] Yue, B., Varadarajan, K.M., Ai, S., Tang, T., Rubash, H.E., Li, G., 2011, Differences of Knee Anthropometry Between Chinese and White Men and Women, *J Arthroplasty.* **26**, pp. 124-130.

[6] Jamali, A.A., Mak, W., Wang, P., Tai, L., Meehan, J.P., Lamba, R., 2013, What is Normal Femoral Head/Neck Anatomy? An Analysis of Radical CT Reconstructions in Adolescents, Clinical Orthopaedics and Related Research **471**, pp. 3581-3587.

[7] Winter, D.A., 2009, *Biomechanics and Motor Control of Human Movement, 3rd edition.* Wiley. Hoboken, NJ.

[8] Murayama, T., Sato, T., Watanabe, S., Kobayashi, K., Tanifuji, O., Mochizuki, T., Yamagiwa, H., Koga, Y., Omori, G., Endo, N., 2016, Three-dimensional in vivo dynamic motion analysis of anterior cruciate ligament-deficient knees during squatting using geometric center axis of the femur, Journal of Orthopaedic Science **21**, pp. 159-165.

[9] Murakami, K., Hami, K., Okazaki, K., Ikebe, S., Shimoto, T., Hara, D., Mizu-uchi, H., Higaki, H., Iwamoto, Y., 2016, *In vivo* kinematics of healthy male knees during squat and golf swing using image-matching techniques, The Knee **23**, pp. 221-226.

[10] Shelburne, K.B., Pandy, M.G., 1998, Determinants of cruciate-ligament loading during rehabilitation exercise, Clinical Biomechanics **13**, pp. 403-413.

[11] Toutoungi, D.E., Lu, T.W., Leardini, A., Catani, F., O'Connor, J.J., 2000, Cruciate ligament forces in the human knee during rehabilitation exercises, Clinical Biomechanics **15**, pp. 176-187.